Available online at www.sciencedirect.com
ScienceDirect
Ceramics International 35 (2009) 559–564
CERAMICS INTERNATIONAL
www.elsevier.com/locate/ceramint

Non-isothermal crystallization kinetics and microwave properties of $Bi_{0.75}Y_{2.25}Fe_5O_{12}$ prepared by coprecipitation

Yen-Pei Fu [a,*], Dung-Shing Hung [b], Chih-Wen Cheng [a], Feng-Yi Tsai [a], Yeong-Der Yao [c]

[a] Department of Materials Science and Engineering, National Dong Hwa University, Shou-Feng, Hualien 974, Taiwan
[b] Department of Information & Telecommunications Engineering, Ming Chuan University, Taipei 111, Taiwan
[c] Department of Materials Engineering, Tatung University, Taipei 104, Taiwan

Received 15 October 2007; received in revised form 21 November 2007; accepted 7 January 2008
Available online 8 April 2008

Abstract

The non-isothermal crystallization kinetics of $Bi_{0.75}Y_{2.25}Fe_5O_{12}$ powder prepared by coprecipitation has been investigated. The activation energy of crystallization was calculated by differential scanning calorimetry (DSC) at different heating rates. Analysis of non-isothermal DSC data presented values of 650 kJ/mol and 2.48 for the activation energy of crystallization and the Avrami exponent, respectively. This Avrami exponent value was consistent with surface and internal crystallizations occurring simultaneouly. The complex permittivity and permeability of $Bi_{0.75}Y_{2.25}Fe_5O_{12}$ were measured at X-band (8–12 GHz) by cavity perturbation technique. For dielectric properties, the real part of permittivity, ε', was obtained in the range of 13.18–15.28. For magnetic properties, the real part of permeability, μ', was obtained in the range of 12.21–20.98.

Keywords: A. Powders: chemical preparation; C. Magnetic properties; C. Thermal properties; E. Soft magnets

1. Introduction

Yttrium iron garnet (YIG) was extensively studied owing to its interesting physical properties. For example, this material possesses the highest quality factor in microwave regime, and the smallest linewidth in magnetic resonance among magnetic materials [1,2]. YIG-based materials are important components of electronics products, such as circulators, oscillators, and phase shifters. However, YIG is hardly used in multilayer microwave components because of its high sintering temperature (>1350 °C). The sintering temperature of YIG is generally higher than the melting point of highly conductive metals such as Ag–Pd alloy (1145 °C) [3]. Previous investigation have shown that Bi-substituted and 2Ca–V-substituted YIG powders can be prepared at much lower temperatures (<1100 °C) than for preparing YIG due to their lower melting temperature of substitution, and the sintering temperature of these materials is much lower than YIG polycrystalline ceramics [4–6]. The basic property for evaluating magnetic ceramics for microwave application is their low power loss. Accordingly, low dielectric losses are required to increase skin depth so as to ensure that microwaves can penetrate a large volume of magnetic ceramics. A loss tangent on the order of $<10^{-3}$ is desirable for microwave devices such as a phase shifter, an isolator, and a circulator.

Magnetic fine particles are very attractive for magnetic ceramics research. This is due to the fact that they are single magnetic domain and their mutual interaction can be studied without magnetic domain effects. Polycrystalline YIG and substituted-YIG have attracted much attention for microwave devices and magneto-optical applications [7]. The conventional method of producing these materials is by the solid-state reaction with oxide/carbonate and calcination at a high temperature (≧1200 °C). The solid-state reaction method has some inherent disadvantages as follows: (1) chemical inhomogeneity; (2) coarser particle size; and (3) introduction of impurities during ball milling. In order to improve the performance and quality of Bi-YIG magnetic ceramics, coprecipitation is an alternative method to overcome the deficiencies in the conventional solid-state reaction. In general, YIG-based powder can be prepared by using several chemical approaches such as sol–gel [8–11], sol–gel auto combustion method [12,13], spray pyrolysis process [14], and citrate

* Corresponding author. Tel.: +886 3 863 4209; fax: +886 3 863 4200.
E-mail address: d887503@alumni.nthu.edu.tw (Y.-P. Fu).

0272-8842/$34.00
doi:10.1016/j.ceramint.2008.01.005

method [15]. In previous works, there have been many investigations on the microwave and magneto-optical properties, and they have focused on correlations between the microstructure, composition, and magnetic properties of Bi-substituted YIG. Therefore, in this study, we used coprecipitation to produce as-precipitated amorphous $Bi_{0.75}Y_{2.25}Fe_5O_{12}$ powder and investigated its crystallization behavior. Moreover, we also investigated permittivity, permeability, and loss tangent measured at an X-band microwave frequency by a cavity perturbation technique [16,17].

2. Experimental procedures

2.1. Preparation of Bi-YIG powders

Fig. 1 plots the preparation of Bi-YIG particles by coprecipitation. The preparation details are described as follows. According to the stoichiometric composition of $Bi_{0.75}Y_{2.25}Fe_5O_{12}$, specified amounts of bismuth nitrate pentahydrate [$Bi(NO_3)_3{\cdot}5H_2O$], yttrium nitrate hexahydrate [$Y(NO_3)_3{\cdot}6H_2O$], and iron nitrate nonahydrate [$Fe(NO_3)_3{\cdot}9H_2O$] were dissolved in a certain quantity of water. The 28% ammonia solution (NH_4OH) was added rapidly into the stirred solution at room temperature. In the pH range of more than 8.7, the ratio of the cations in the powders was the same as that in the nitrate solution. In this study, the pH of the solution was controlled to be above 12. The obtained slurry was washed with alcohol to remove the alkaline ions and obtain a weak agglomeration of Bi-YIG powders, filtered and dried at 90 °C for 24 h. Then, the coprecipitate of the as-prepared $Bi_{0.75}Y_{2.25}Fe_5O_{12}$ powder was annealed at 700 °C for 2 h. This powder was mixed with 3% polyvinyl alcohol (PVA) binder and pressed into disks, which were sintered at 1050 °C for 2 h in air. A disk was cut into a thin slab for microwave measurement.

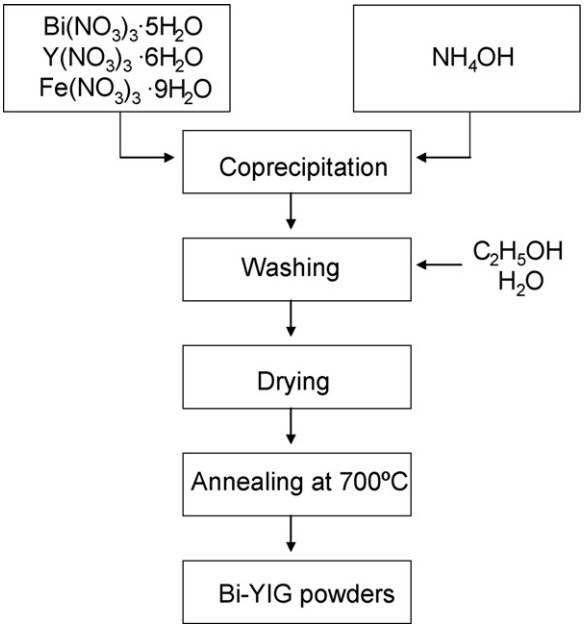

Fig. 1. Flow chart for preparation of $Bi_{0.75}Y_{2.25}Fe_5O_{12}$ particle by coprecipitation.

2.2. Characterization

Differential scanning calorimetry (DSC; Model TG-DTA/DSC Setaram, Caluiro, France) was used to carry out for the crystallization characterization of as-prepared Bi-YIG powders. A heating rate range of 10–25 °C/min was used in DSC measurement up to 900 °C in air. Thermal analysis was carried out under flowing air at 100 ml/min. A constant sample weight of 12.0 ± 0.2 mg was used for all measurements. In this study, DSC instrument was calibrated using Sn. The melting temperature and latent heat of transformation for Sn are 231.8 °C and 60.46 J/g, respectively. The peak area values and onset temperatures were determined by a test run. These values were inputted and calculated by the software. It automatically revealed the correction data. We can use this correction data to correct our future data collected by the instrument. BET surface area measurements were made by nitrogen adsorption employing a Micromeritics ASAP 2020 instrument (Norcross, GA, U.S.A.) and calculated using the five-point Brunauer–Emmit–Teller (BET) theory. Mean particle size (D_{BET}) was calculated from the BET data according to the following equation assuming that the particles are closed sphere with smooth surface and uniform size: $D_{BET} = 6 \times 10^3/(\rho_{th}\ S_{BET})$, where D_{BET} (nm) is the average particle size, S_{BET} is the measured specific surface area expressed in m^2/g and ρ_{th} is the theoretical density of the compound (g/cm^3). The magnetic properties of Bi-YIG powders at room temperature were measured by a vibrating sample magnetometer (VSM; Model 7407 Lake Shore, Westerville, OH, U.S.A.).

Cavity perturbation technique has been used for the measurements of the complex permittivity and permeability of Bi-YIG at microwave frequencies in this study. The cavity used was made from the standard copper waveguide and had the dimension as shown in Fig. 2. It was conducted to a network analyzer (Model Agilent 8510C, Santa Clara, CA, U.S.A.) and excited into several modes. Thin Bi-YIG slabs were placed straight through the slot in the cavity. Measurements and calculations were made according to the procedure described elsewhere [16–18].

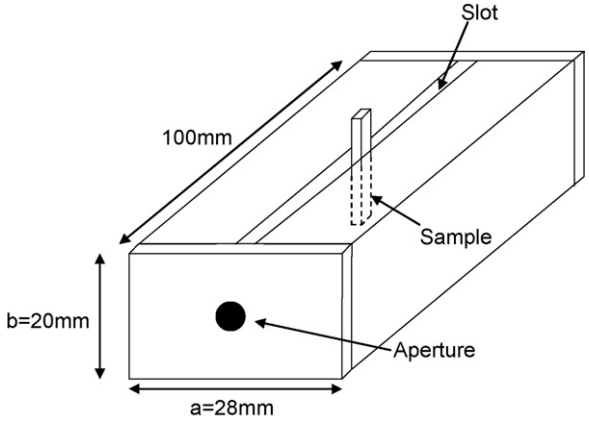

Fig. 2. Rectangular cavity resonator with dimensions $L = 100$, $a = 28$, and $b = 20$ mm. The slot is $90 \times 5\ mm^2$, and the sample dimension is $15 \times 5 \times 1.5\ mm^3$.

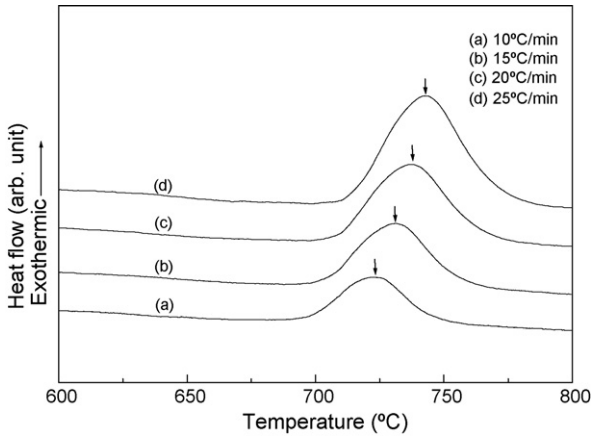

Fig. 3. Differential scanning calorimetry curves of as-prepared $Bi_{0.75}Y_{2.25}Fe_5O_{12}$ powders at different heating rates of 10, 15, 20, and 25 °C/min.

3. Results and discussion

Crystallization characterization of the Bi-YIG powder was estimated by non-isothermal DSC. Fig. 3 shows the DSC curves of a sample at different heating rates ranging from 10 to 25 °C/min. With increasing heating rate, the exothermic peak shifts to a higher temperature. The X-ray diffraction (XRD) patterns of heat-treated samples at different temperatures of 600–675 °C for 2 h are presented in Fig. 4. The broad low-intensity peak is indicative of the amorphous nature of the powder for $Bi_{0.25}Y_{2.75}Fe_5O_{12}$ specimen. This broad low-intensity peak is observed at 32° diffraction angle. When the heat-treated temperature reached 625 °C, the specimen revealed (4 0 0), (4 2 0), and (4 2 2) low-intensity peaks. With increasing heat-treated temperature, the number of broad hump associated with the amorphous phase decreased, and the intensity of XRD peaks increased as the amorphous phase transformed into the crystalline phase, the garnet phase. The volume fraction of the crystallized phase increases with increasing heat-treated temperature. These results are consistent with the DSC results. The specific surface area and mean particle size of Bi-YIG powders calcined at different temperatures are listed in Table 1.

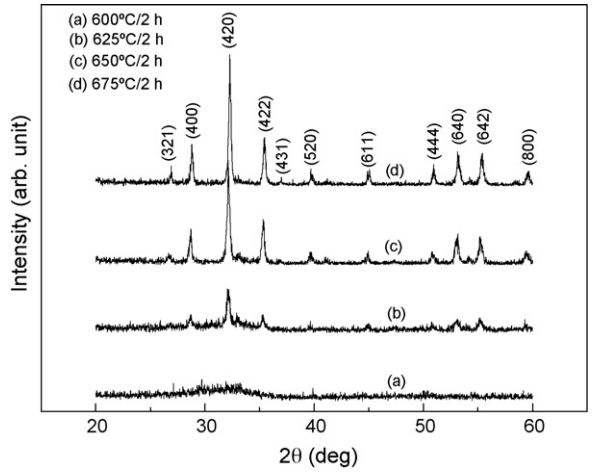

Fig. 4. X-ray diffraction results of powders calcined at various temperatures for 2 h.

Table 1
Specific surface area and mean particle size for $Bi_{0.75}Y_{2.25}Fe_5O_{12}$ materials after calcinations at different temperatures

Calcination temperature (°C)	Surface area (m^2/g)	Mean particle size[a] (nm)
600	46	22
625	37	27
650	17	59
675	10	104

[a] Mean particle size measured from specific surface area.

The result indicates that the particle size increased with annealing temperature. Compared XRD with BET results, we can conclude that when garnet crystalline phase appears, the mean particle size requires larger than 28 nm prepared by coprecipitation process.

The crystallization peaks depending on the DSC scan rates can be used to estimate the activation energy of crystallization. The activation energy value for the crystallization can be estimated using following Kissinger analysis [19]. Through the change in the peak crystallization temperature (T_p) with respect to heating rate, the activation energy of crystallization could be determined using the Kissinger equation as follows:

$$\ln\left(\frac{T_p^2}{\Phi}\right) = \frac{E}{RT_p} + \text{constant} \quad (1)$$

where E is the activation energy of crystallization. T_p is the temperature corresponding to the maximum of the DSC crystallization peak, R is the gas constant (8.314 J/mol), and Φ is the heating rate. The Φ used are 10, 15, 20, and 25 °C/min. If the slope of the plot of $\ln(T_p^2/\Phi)$ versus $1/T_p$ is a straight line, and the slope is E/R, the activation energy of the crystallization could be estimated. Fig. 5 shows the Kissinger plot of the as-prepared $Bi_{0.75}Y_{2.25}Fe_5O_{12}$ powder. The activation energy of crystallization is determined using the Kissinger equation from the slope and is equal to 377 kJ/mol.

Moreover, the Avarami exponent n can be determined from the DSC results. The value of the Avrami parameter n, which is a measure of the dimensionality of transformation, is

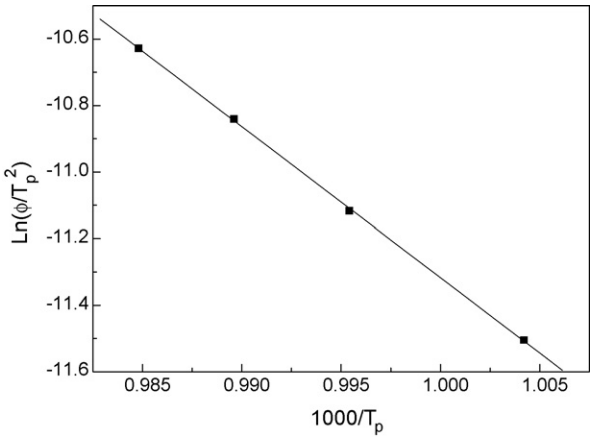

Fig. 5. Plot of $\ln(T_p^2/\Phi)$ against $1/T_p$ for determining the value of crystallization activation energy of $Bi_{0.75}Y_{2.25}Fe_5O_{12}$.

determined using the Ozawa equation [20]:

$$\frac{d\{\ln[-\ln(1-X)]\}}{d\ln\Phi} = -n \quad (2)$$

where Φ is the different heating rates, X is the volume fraction crystallized at a specified temperature T, X is the given ratio of the partial area crystallized at a certain temperature to the total area of the crystallization exotherm. Here, the total area of the crystallization exotherm is between the temperature T_i at which crystallization just begins and the temperature T_f at which the crystallization is complete. The partial area crystallized at a certain temperature is between T_i and T [21]. A plot of $\ln[-\ln(1-X)]$ versus $\ln\Phi$ should be a straight line from the slope, which n can be calculated. An n close to 3 indicates bulk or three-dimensional crystal growth and an n close to 1 indicates surface growth. Intermediate values of n between 1 and 3 indicate that surface and internal crystallizations occur simultaneously [22]. The Ozawa plot of $\ln[-\ln(1-X)]$ versus $\ln\Phi$ is shown in Fig. 6. Here, the volume fraction crystallized was calculated at a fixed temperature of 725 °C. The value of n determined from the slope of the plot was 2.48. This result indicates that crystallization is predominated by surface and internal crystallizations occurring simultaneous. Crystallization has a very strong dependence on bulk nucleation with two- to three-dimensional crystal growth.

Matusita and Sakka [23,24] proposed that the Kissinger model is only valid when crystal growth occurs on a specified number of nuclei. They modified the Kissinger equation to account for nucleation and crystallization growth occurring simultaneously to

$$\ln\left(\frac{\Phi^n}{T_p^2}\right) = -\frac{mE_c}{RT_p} + \text{constant} \quad (3)$$

where E_c is the activation energy of crystallization and m represents the dimensionality of the crystalline phase. n and m are correlated to each other through the relation $m = n - 1$. Fig. 7 show the Matusita and Sakka plot for the determined of crystal growth activation energy, where m is equal to 1.48. Substituting the value of $n = 2.48$ and $m = 1.48$ into the modified Kissinger equation obtained an activation energy of 650 kJ/mol. Xu et al.

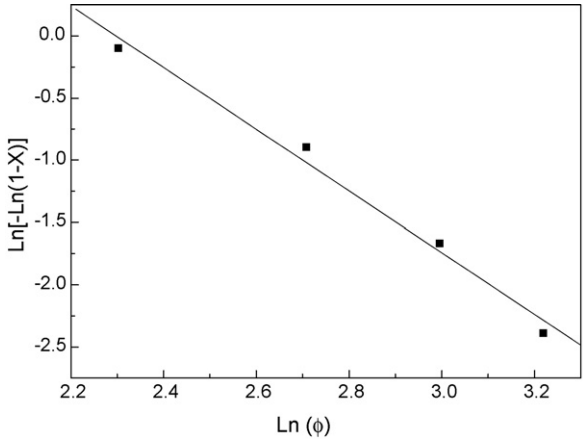

Fig. 6. Plot of $\ln[-\ln(1-X)]$ versus $\ln\Phi$ for determining Avrami constant n.

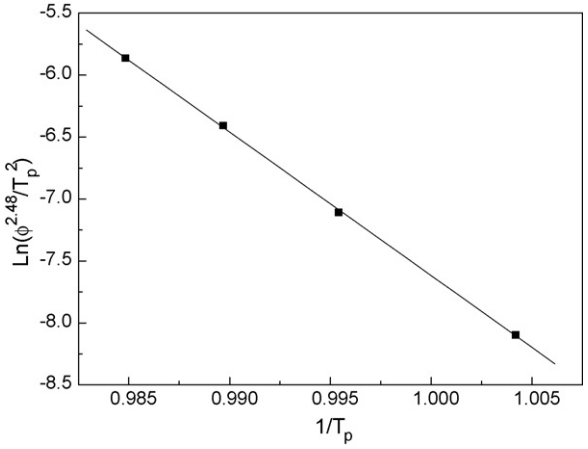

Fig. 7. Plot in accordance with Matusita and Sakka equation for determination of activation energy of crystallization.

[25] and Yinnon and Uhlmann [26] proposed a simple method to obtain a modified activation energy of crystallization. Multiplying E_c from the Kissinger plot in Eq. (1) by the factor n/m yields 632 kJ/mol, which is approximately consistent with the value determined using Eq. (3) and with an error of less than 3%. Therefore, we can estimate the activation energy of crystallization by this simple method.

The magnetization measurements for the $Bi_{0.75}Y_{2.25}Fe_5O_{12}$ powder prepared by the coprecipitation were carried out using a vibrating sample magnetometer (VSM) at room temperature with an applied magnetic field of 10 kOe to reach the saturation value. Fig. 8 shows a hysteresis loop for the $Bi_{0.75}Y_{2.25}Fe_5O_{12}$ powder. This figure indicates that Bi-YIG is a soft magnetic material. The $Bi_{0.75}Y_{2.25}Fe_5O_{12}$ powder prepared by coprecipitation followed annealing at 700 °C for 2 h with a saturation magnetization (M_s) of 23.01 emu/g, a remanence (M_r) of 2.24 emu/g, and an intrinsic coercive force (H_{ci}) of 26.56 Oe. The permittivity, permeability, and loss tangent value at X-band microwave frequencies of 8.053, 8.9288, 9.9820, and 11.0924 GHz for $Bi_{0.75}Y_{2.25}Fe_5O_{12}$ is presented in Table 2.

At microwave frequency, the interfacial and dipolar polarization effects will be largely absent, the dielectric

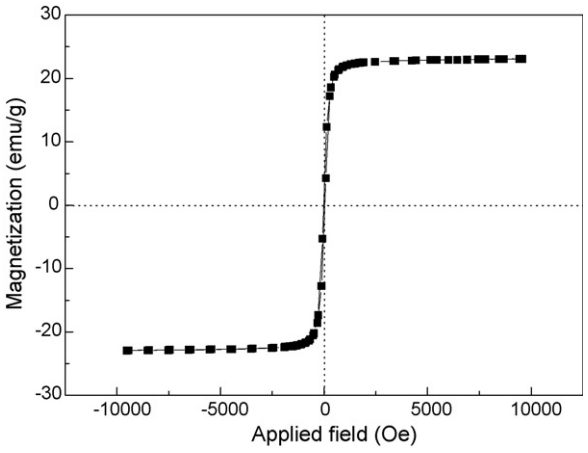

Fig. 8. Magnetization against applied field hysteresis for as-prepared $Bi_{0.75}Y_{2.25}Fe_5O_{12}$ powder annealed at 700 °C for 2 h.

Table 2
Complex permittivity, permeability, and loss factor at X-band microwave frequencies for $Bi_{0.75}Y_{2.25}Fe_5O_{12}$ magnetic ceramic sintered at 1050 °C

Frequency (GHz)	ε'	ε''	tan δ_e	μ'	μ''	tan δ_m
8.057	13.188	0.0124	0.000945	20.980	0.0408	0.001947
8.928	14.371	0.0070	0.000491	16.253	0.0161	0.000991
9.982	14.829	0.0085	0.000577	13.586	0.0155	0.001147
11.092	15.280	0.0057	0.000374	12.207	0.0089	0.000734

constant is mainly contributed by the atomic and electronic polarizations in the garnet grains. Variations in dielectric constant of garnets have mainly been attributed to the variations in the concentration of Fe^{2+} ions [27,28]. The ε' values were obtained in the range of 13.18–15.28, and ε'' was observed to lie in the range of 0057–0.0124. Dielectric loss in polycrystalline garnets is due to the lag in polarization in the alternating electric field. This lag increases due to the presence of impurities and imperfections in the garnet structure. The permittivity losses, tan $\delta_e(=\varepsilon''/\varepsilon')$, obtained in the present work are in the order of 10^{-3}–10^{-5}. At microwave frequencies, permeability of garnet is mainly contributed by spin rotation. When excited by an applied alternating magnetic field, the magnetization vector will precess around the anisotropy field. According to previous literatures [29], in the presence of an external RF field, the real part μ' can be expressed as follows,

$$\mu' = \left[\frac{\omega_P^2}{\omega_P^2 - \omega^2 + jd\omega}\right]\varepsilon\cos\,\omega t$$

where ω_p is the Larmor frequency, ω is the frequency of the alternating field, ε is the precessional angle, and $jd\omega$ is s damping term with d as the damping factor, which depends upon the damping of the precessional motion due to inhomogeneities and imperfections in the crystal lattice. When $\omega_p = \omega$, μ' increases gradually as ω increases. When $\omega_p = \omega$, a maximum μ' is obtained and when $\omega_p < \omega$, the magnetization vector and the RF magnetic field get out of phase, μ' suddenly falls and changes sign and become negative. This phenomenon is known as resonance. Resonance occurs when the frequency of the applied field coincides with the natural precessional frequency [30]. The μ' value was obtained in the range of 12.21–20.98, μ'' was observed to lie in the range of 0.0089–0.0408. The permittivity loss, tan $\delta_m(=\mu''/\mu')$, was obtained in the range of 1.94×10^{-3}–7.34×10^{-4}.

4. Conclusions

A non-isothermal study of the crystallization kinetic of coprecipitation $Bi_{0.75}Y_{2.25}Fe_5O_{12}$ was carried out by DSC. The activation energy of crystallization is determined using the method proposed by Kissinger from the slope and is equal to 377 kJ/mol. The Avrami exponent n suggesting the dimensionality of crystal growth was determined using the Ozawa equation. In this study, n was equal to 2.48 which indicates surface and internal crystallization occurring simultaneously. By applying the modified Kissinger model, the activation energy of crystallization was found to be 650 kJ/mol. The complex permittivity and permeability of $Bi_{0.75}Y_{2.25}Fe_5O_{12}$ were measured at X-band (8–12 GHz) by the cavity perturbation technique. For dielectric properties, the real part of permittivity, ε', was in the range of 13.18–15.28. For magnetic properties, the real part of permeability, μ', was in the range of 12.21–20.98.

Acknowledgement

The author would like to thank the National Science Council of the Republic of China for financially supporting this research under Contract No. NSC 96-2221-E-259-005.

References

[1] Z. Yue, L. Li, J. Zhou, H. Zhang, Z. Ma, Z. Gui, Preparation and electromagnetic properties of ferrite-cordierite composites, Mater. Lett. 44 (2000) 279–283.
[2] H.M. Sung, C.J. Chen, W.S. Ko, H.C. Lin, Fine powder ferrite for multilayer chip inductors, IEEE Trans. Magn. 30 (1994) 4906–4908.
[3] H. Zhao, J. Zhou, Y. Bai, Z. Gui, L. Li, Effect of Bi-sbubstitution on the dielectric properties of polycrystalline yttrium iron garnet, J. Magn. Magn. Mater. 280 (2004) 208–213.
[4] S. Geller, H.J. Williams, G.P. Espinosa, R.C. Sherwood, M.A. Gilleo, Reduction of the preparation temperature of polycrystalline garnets by bismuth substitution, Appl. Phys. Lett. 3 (1963) 21–22.
[5] K. Shinagawa, S. Taniguchi, Faraday effect of Bi-substituted rare-earth iron garnet, Jpn. J. Appl. Phys. 12 (1973), 465–465.
[6] Y.Y. Song, S.C. Yu, W.T. Kim, J.R. Park, T.H. Kim, The effect of Bi_2O_3 addition on the microstructure and magnetic properties of YIG, J. Magn. Magn. Mater. 256 (1998) 177–181.
[7] N. Kawai, E. Komuro, T. Namikawa, Y. Yamazaki, Preparation of Bi-YIG particles for display devices, IEEE Trans. Magn. 30 (1994) 4446–4448.
[8] Z. Cheng, H. Yang, L. Yu, Y. Cui, S. Feng, Preparation and magnetic properties of $Y_3Fe_5O_{12}$ nanoparticles doped with the gadolinium oxide, J. Magn. Magn. Mater. 302 (2006) 259–262.
[9] V. Sankaranarayanan, N.S. Gajbhiye, Low-temperature preparation of ultrafine rare-earth iron garnets, J. Am. Ceram. Soc. 73 (1990) 1301–1307.
[10] C.S. Kuroda, T. Tanniyama, Y. Kitamoto, Y. Yamazaki, Magneto-optical properties and morphology of particulate film consisting of Bi-YIG coprecipitated Particles, J. Magn. Magn. Mater. 241 (2002) 201–206.
[11] E. Garskaite, K. Gibson, A. Leleckaite, J. Glaser, D. Niznasky, A. Kareiva, H.J. Meter, On the synthesis and characterization of iron-containing garnet ($Y_3Fe_5O_{12}$, YIG and $Fe_3Al_5O_{12}$, IAG), Chem. Phys. 323 (2006) 204–210.
[12] S.H. Vajargah, H.R.M. Hosseini, Z.A. Nemati, Preparation and characterization of yttrium iron garnet (YIG) nanocrystalline powders by autocombustion of nitrate-citrate gel, J. Alloys and Compd. 430 (2007) 339–343.
[13] S.H. Vajargah, H.R.M. Hosseini, Z.A. Nemati, Synthesis of nanocrystalline yttrium iron garnet by sol–gel combustion process: the influence of pH of precursor solution, Mater. Sci. Eng. B 129 (2006) 211–215.
[14] D.S. Todorovsky, R.V. Todorovska, St. Groudeva-Zotova, Thermal decomposition of yttrium-iron citrates preparation in ethylene glycol medium, Mater. Lett. 55 (2002) 41–45.
[15] K. Matsumoto, K. Yamaguchi, T. Fujii, A. Ueno, Preparation of bismuth-substituted yttrium iron garnet powders by the citrate gel process, J. Appl. Phys. 69 (1991) 5918–5920.

[16] U. Raveendranath, K.T. Mathew, New cavity perturbation technique for measuring complex permeability of ferrite materials, Microwave Opt. Technol. Lett. 18 (1998) 241–243.
[17] M. Hajian, K.T. Mathew, L.P. Lighart, Measurement of complex permittivity with waveguide resonator using perturbation technique, Microwave Opt. Technol. Lett. 21 (1999) 269–272.
[18] A. Verma, D.C. Dube, Processing of nickel-zinc ferrite via the citrate precursor route for high-frequency applications, J. Am. Ceram. Soc. 88 (2005) 519–523.
[19] H.E. Kissinger, Variation of peak temperature with heating rate in different thermal analysis, J. Res. Natl. Bur. Stand. (U.S.) 57 (1956) 217–221.
[20] T. Ozawa, Kinetic of non-isothermal crystallization, Polymer 12 (1971) 150–158.
[21] C.T. Cheng, M. Lanagan, B. Jones, J.T. Lin, M.J. Pan, Crystallization kinetic and phase development of PbO-BaO-SrO-Nb_2O_5-B_2O_3-SiO_2-based glass-ceramics, J. Am. Ceram. Soc. 88 (2005) 3037–3042.
[22] A.A. Francis, Non-isothermal crystallization kinetics of a blast furnace slag glass, J. Am. Ceram. Soc. 88 (2005) 1859–1863.
[23] K. Matusita, S. Sakka, Kinetics study of crystallization of glasses by differential scanning calorimeter, Phys. Chem. Glasses 20 (1979) 81–84.
[24] K. Matusita, S. Sakka, Kinetics study on crystallization of glass by differential thermal analysis-criterion on application of Kissinger plot, J. Non-Cryst. Solids 38–39 (1980) 741–746.
[25] X.J. Xu, C.S. Ray, D.E. Day, Nucleation and crystallization of Na_2O-2CaO-3SiO_2 glass by differential thermal analysis, J. Am. Ceram. Soc. 74 (1991) 909–914.
[26] H. Yinnon, D.R. Uhlmann, Application of thermoanalytical techniques to study of crystallization kinetics in glass-forming liquids. Part I. Theory, J. Non-Cryst. Solids 54 (1983) 253–275.
[27] J.T.S. Irvine, A. Huanosta, R. Velenzuela, A.R. West, Electrical properties of polycrystallines nickel zinc ferrites, J. Am. Ceram. Soc. 73 (1990) 729–732.
[28] C.G. Koops, On the dispersion of resistivity and dielectric constant of some semiconductors at audio frequencies, Phys. Rev. 83 (1951) 121–124.
[29] H.G. Belegers, J.L. Snoek, Gyromagnetic phenomena occurring with ferrites, Philips Tech. Rev. 11 (1950) 313–340.
[30] A.J. Moulson, J.M. Herbert, Electroceramics: Materials, Properties and Applications, Chapman & Hall, London, 1990.